JOURNAL OF MATERIALS SCIENCE 5 (1970) 275–282

The Structure of Epitaxial Films of ZnS Evaporated onto NaCl in a Vacuum

D. B. HOLT,* J. M. WOODCOCK†
Department of Metallurgy, Imperial College, London SW7, UK

The defect structures of epitaxial films of ZnS evaporated onto NaCl in vacuum were studied by transmission electron microscopy. Included grains of doubly-positioned wurtzite-structure material were found in many of the monocrystalline sphalerite-structure films. No twins or wurtzite grains in other orientations were ever observed.

Numerous {111} planar defects were present in the films that were grown free of included grains. Interaction between doubly diffracted electron beams, arising from the ⟨111⟩ streaks due to the planar defects and the direct beam produced characteristic systems of fine-scale fringes and dots which dominated the appearance of the micrographs. Annealing in vacuum and in H_2S failed to eliminate the planar defects.

1. Introduction

In an earlier paper it was reported that focused electron beam evaporation in ultra-high vacuum onto vacuum-cleaved NaCl substrates produced epitaxial films of ZnS that were free of included grains of second phase material and free of microtwins [1]. Subsequently it was shown that a number of deviations from optimum growth conditions, especially the use of hot metal evaporators, too high deposition rates (greater than 200 Å sec^{-1}), and poor vacuum, resulted in the incorporation of doubly-positioned wurtzite-structure (hexagonal) material in the sphalerite (cubic) films. Co-evaporation of either Zn or S with ZnS produced cubic films, large areas of which contained wurtzite grains in only one of the two positions. It was also shown that the single-phase single crystal ZnS films gave reproducible current-voltage characteristics which were interpreted as due to thermionic emission of carriers over field-lowered contact barriers (the Schottky effect) [2].

In the present paper detailed evidence on the structure of the included grains in the less perfect films is presented, and an account is given of the contrast arising from the most important remaining type of defect in the films that were grown free of included grains.

2. Experimental Methods

ZnS films were epitaxially grown on vacuum-cleaved faces of NaCl by focused electron beam evaporation in high and ultra-high vacua as previously described [1, 2]. The films were floated off the substrates in water and examined by transmission electron microscopy.

After removal from their substrates some films were mounted on gold grids to avoid contamination during annealing. Some of these films were annealed in vacuum. This was done in the substrate heater of the vacuum system in which they had been grown. Other films were placed in silica boats and inserted in a furnace inside a glass system which could be flushed and then filled with H_2S at a pressure of 1 atm.

3. Results

3.1. Included Grains

The most prominent feature of epitaxial films of ZnS grown on NaCl in less than the most clean conditions was the occurrence of included grains giving rise to satellite spots in the diffraction pattern which could all be indexed in terms of doubly-positioned wurtzite-structure grains as indicated in fig. 1 [2]. These grains all occur with the (0001) basal plane parallel to the (100) plane of the cubic matrix of the film. The

*Temporary address: School of Physics, University of New South Wales, Kensington, NSW, Australia.
†Present address: Mullard Research Laboratories, Salfords, Nr. Redhill, Surrey, UK.

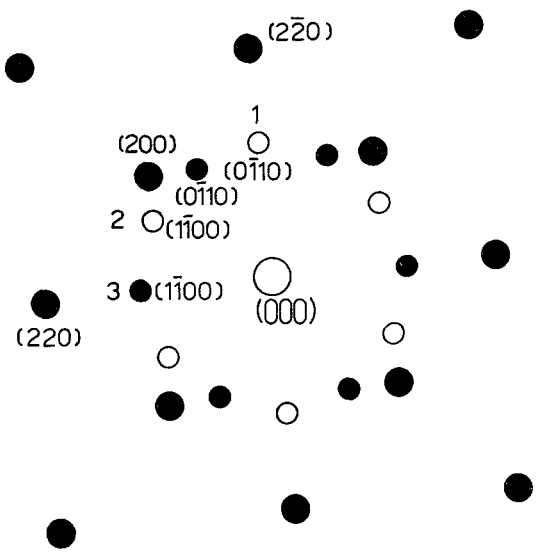

Figure 1 (100) sphalerite reciprocal lattice plane with satellites arising from wurtzite-structure included grains having (0001) parallel to the (100) plane of the sphalerite matrix and occurring in two positions rotated by 30° to one another about the [100] axis. The large solid circles with cubic (3 digit) indices represent the sphalerite diffraction spots. The smaller circles with hexagonal (4 digit) indices represent the wurtzite satellite spots; the small open circles arise from grains in the one position and the small solid circles from grains in the other position. Satellites arising from sphalerite-structure grains having (211) parallel to the sphalerite matrix (100) plane and occurring in six positions related by rotations of 30° about the [100] axis would occur in the same positions. Satellites 1 and 2 arise from the same grains on the doubly-positioned wurtzite interpretation and from different grains in the latter interpretation.

one position has [2$\bar{1}\bar{1}$0] wurtzite parallel to [110] sphalerite, while the other position is rotated through 30° about the film normal relative to the first, and has [1$\bar{2}$10] wurtzite parallel to [1$\bar{1}$0] sphalerite. Additional satellite spots displaced by $\pm$ 1/3 ⟨111⟩ and $\pm$ 1/6 ⟨111⟩ from the cubic matrix spots are to be expected when microtwins and grains of hexagonal material occur on the {111} planes of the cubic matrix [3-5]. However none of these satellite spots, ascribable to microtwins or to wurtzite in orientations other than the doubly-positioned ones, were ever observed, nor were included grains, other than doubly-positioned wurtzite, ever seen. A possible alternative interpretation of the satellite spots indicated in fig. 1 had to be considered however. Aggarwal and Goswami [6] in an electron diffraction study of films of ZnS, interpreted certain of their observations in terms of multiply-positioned {211} cubic (sphalerite) included grains. If the (100) sphalerite films contained included grains of (211) sphalerite material in six positions related by incremental rotations of 30° about the [100] film normal, these grains would give rise to satellite spots at positions very near those due to doubly-positioned wurtzite grains. However, the two interpretations differ as indicated on fig. 1 in that alternate beams arise from the same grains on the doubly-positioned wurtzite interpretation, but from different grains on the multiply-positioned twinned sphalerite interpretation. Dark field microscopy showed that the alternate beams did arise from the same grains, as fig. 2 shows. The included grains were therefore of the doubly-positioned wurtzite-structure.

Confirmation of this interpretation was provided by observations on films grown by co-evaporating ZnS with a non-stoichiometric excess of either Zn or S. In these films only one of the two sets of alternating beams were present as can be seen in fig. 3. The absence of the second set of satellites was confirmed by tilting. The absence of one set of satellites would make no sense on the multiply-positioned {211} sphalerite interpretation. Dark field microscopy with the aperture placed where a satellite beam of the second set would occur, confirmed that no wurtzite grains of that position were present in these films.

3.2. Planar Defects

The films grown under the cleanest conditions were free of included grains and no satellite spots appeared in their diffraction patterns [1, 2]. The diffraction patterns from films of ZnS free of included grains however were prominently streaked in the ⟨111⟩ directions. This is shown in fig. 4 in a diffraction pattern from a (100) film tilted so that the electron beam was incident in a ⟨110⟩ direction. Microdensitometer traces confirmed that there were no intensity maxima, due to microtwins or wurtzite grains [3-5], along the streaks.

Except in certain special orientations of the films relative to the incident electron beam, such as that just discussed, only parts of the streaks appeared. In terms of the Ewald diffraction construction, these parts corresponded to the positions where the sphere of reflection intersected the continuous streaks in reciprocal space.

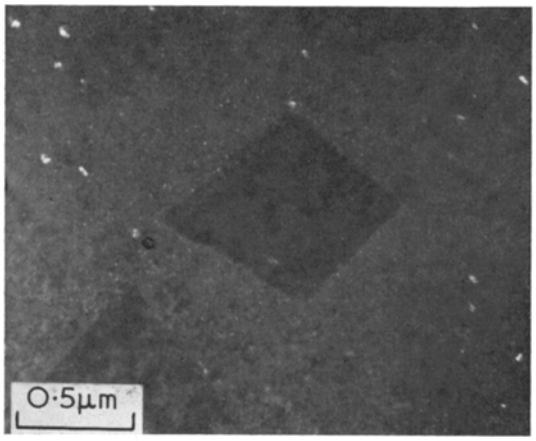

(a)

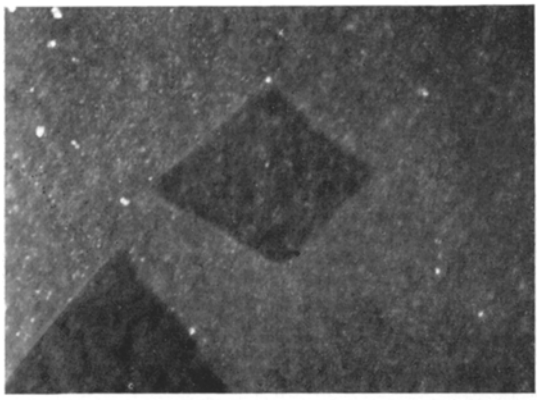

(b)

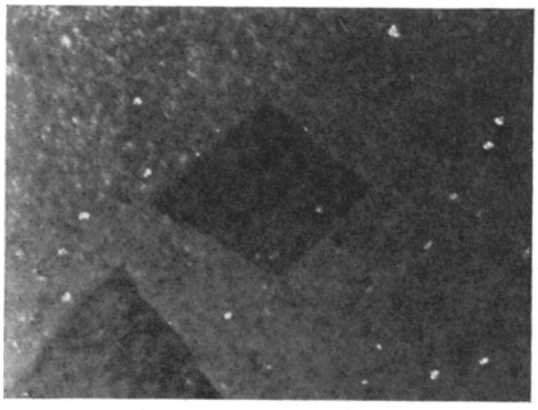

(c)

Figure 2 Dark field transmission electron micrographs of the same area of an epitaxial film of ZnS taken with the satellite beams numbered in fig. 1: (a) beam 1 (b) beam 2 (c) beam 3. The satellites therefore arise from doubly-positioned grains.

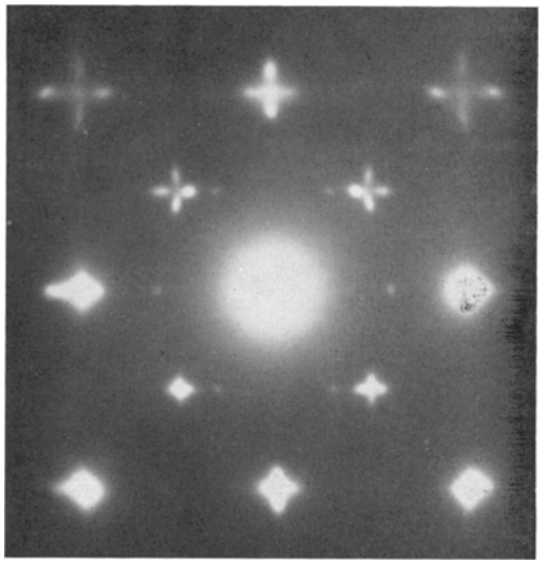

Figure 3 Diffraction pattern of a film grown by co-evaporating ZnS and excess S. Beams are present from only one of the two wurtzite positions plotted in fig. 1.

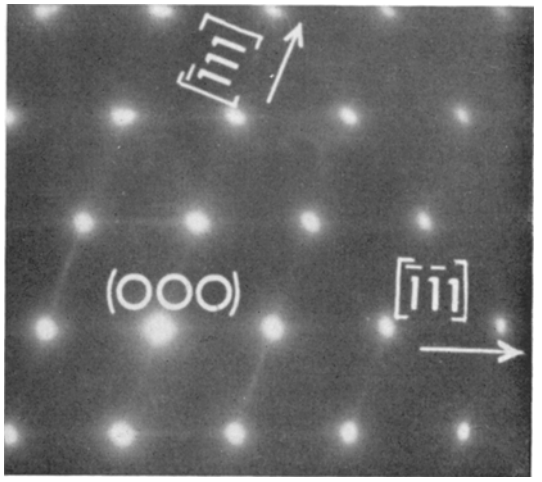

Figure 4 (110) diffraction pattern from a (100) film of epitaxial ZnS. The streaks in the ⟨111⟩ directions contained no intensity maxima i.e. no satellite spots occurred.

The result was the appearance of satellite pseudo-spots around the matrix spots. This is illustrated in fig. 5.

Dark field images were formed in the electron microscope using electrons scattered into parts of the diffraction streaks (i.e. into the satellite pseudo-spots). When the incident electron beam was a few degrees from the [001] film normal a high density of triangular or irregular areas were

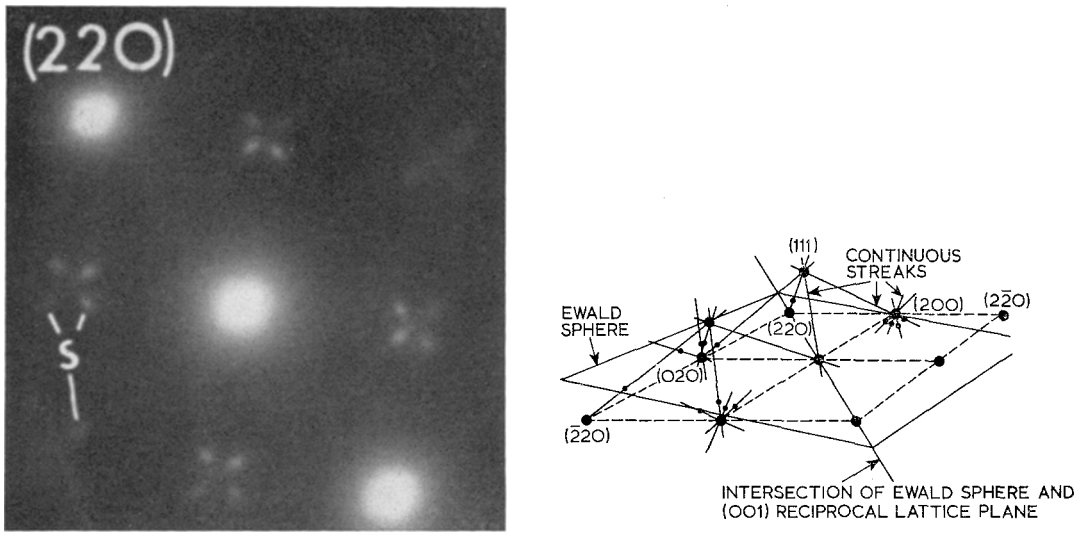

(a) (b)

Figure 5 (a) Transmission electron diffraction pattern from a ZnS film free of included grains with the incident electron beam slightly off the [001] film axis. Some of the satellite pseudo-spots are marked S. (b) The Ewald Sphere diffraction construction for the formation of the satellite pseudo-spots in (a). These occur where the Ewald Sphere intersects the continuous ⟨111⟩ streaks in reciprocal space. Not all of the streaks are shown; ● = pseudo-spots.

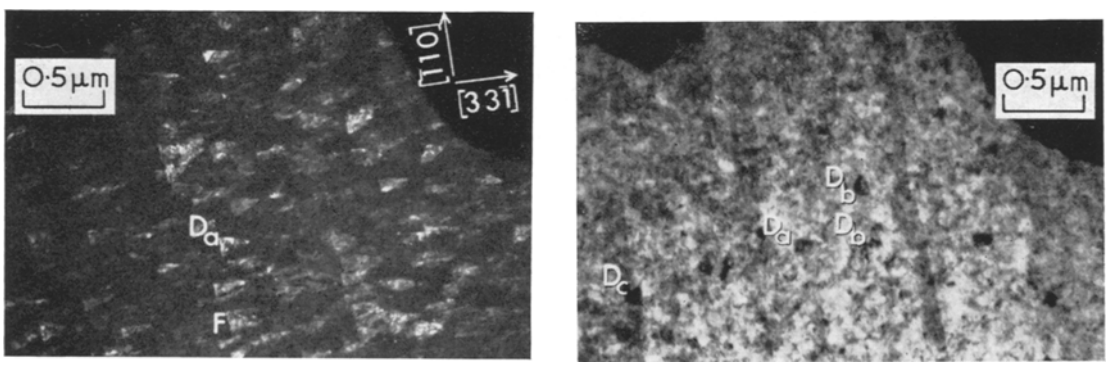

(a) (b)

Figure 6 (a) Dark field micrograph showing triangular planar defects. (b) Bright field image of the same area as shown in (a). Defect D_a is marked in both micrographs. The defects D_b and D_c are triangular defects in different orientations.

observed as shown in fig. 6. Various forms of contrast were visible in the triangles but no clear examples of simple stacking fault fringes were ever recorded. Certain areas of particular defects exhibited fringes, however.

The triangles in fig. 6a in which the electron beam was incident in the [1 1 6] direction all had one edge parallel to the [$\bar{1}$ 1 0] direction. They were of a uniform length of approximately 1900 Å along the [3 3 $\bar{1}$] direction, which was the projected direction in the (1 1 6) plane from the centres of the bases to the apices of the triangles. This is the projected length that would be obtained if the triangular defects lay in the (1 1 1) planes which were inclined 54.7° to the (0 0 1) plane of the film and extended through a film 2000 Å thick. Triangular defects in other orientations are visible in the bright field micrograph of fig. 6b. Dark field images were also formed with the diffraction streaks when the incident electron beam was close to the [1 0 1] axis of the film. The defects were then seen edge-on as bright lines along the [1 2 $\bar{1}$] direction as shown in fig. 7.

Near the (1 0 0) orientation, the Ewald sphere

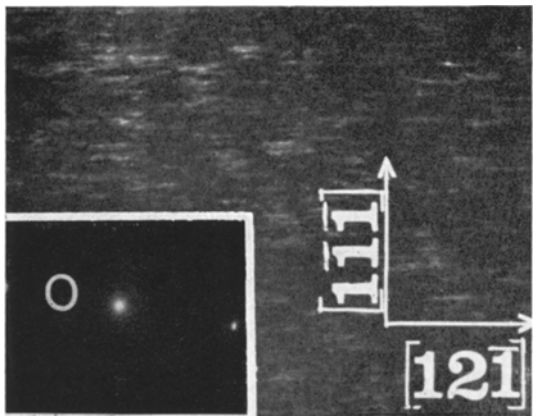

Figure 7 Dark field image of a ZnS film, using part of the diffraction streak as shown in the inset, with the incident electron beam close to the [101] axis.

cuts the ⟨111⟩ streaks in reciprocal space to give rise to sets of four satellite pseudo-spots round the points of the sphalerite diffraction pattern as shown in fig. 5a. Double diffraction will result in a similar set of satellite pseudo-spots round the direct beam. The electron beams of these satellite pseudo-spots should interfere with the direct beam to produce fringes in the micrographs. Fine scale fringe and dot contrast, ascribable to dense, crossed grids of fringes arising from this cause did occur. It was in fact the dominant feature of the most structurally perfect films as shown in fig. 8. The bend extinction contours in the images of these films were of non-uniform contrast and frayed out at the edges. At higher magnifications, square arrays of dots and areas of closely spaced fringes were resolved at the edges of bend contours. It is suggested that the fringes were produced by interference between the transmitted electron wave and an adjacent diffracted wave which had been produced by double diffraction. The first of these diffractions was into a satellite pseudo-spot and a subsequent diffraction produced a spot close to the spot from the transmitted beam. Fringes would then appear in the bright field images perpendicular to the direction between the spot caused by double diffraction and the spot from the transmitted beam, as illustrated in fig. 9. The spacing of the fringes would be the reciprocal of the distance between the two spots in reciprocal space. Overlapping fringes at right angles producing an array of dots would appear when two doubly diffracted spots, with their reciprocal lattice vectors at right angles, were imaged together with the centre spot. Therefore regions of the films in which arrays of dots appeared would have to contain overlapping defects on different {111} planes giving rise to the two ⟨111⟩ streaks producing the two satellite pseudo-spots. Different spacings for the fringes and dots would be produced by local variations in the orientation of the film because the separation of the satellite pseudo-spots from the matrix diffraction spots is sensitive to the orientation (buckling) of the specimen as can be seen in fig. 5b. The range of spacings observed would be limited by both the size of the objective aperture and the resolution of the electron microscope. This means that only satellite pseudo-spots close to the transmitted beam could contribute to the image. Hence the deviation from the exact Bragg condition for a set of planes must be small in order that the sphere of reflection pass near a matrix spot and cut the ⟨111⟩ streaks in nearby points (fig. 5). Therefore fringes would only be observed close to bend extinction contours, where the sphere of reflection passes through matrix points.

The observations were consistent with this interpretation. Fringes were only visible near extinction contours (fig. 8). The fringes were of variable spacing and their visibility was very sensitive to the film orientation and to the conditions of illumination. The orientations of the fringes and, within the limits of experimental

TABLE I Effects of annealing epitaxial films of ZnS.

Temperature	Environment	Changes in diffraction patterns	Changes in micrographs
350° C	vacuum	nil	nil
350° C	H_2S	weak maxima at ± 1/3 ⟨111⟩	nil
450° C	vacuum	nil	nil
450° C	H_2S	increased ± 1/3 ⟨111⟩ maxima	pits formed; some grains visible
550° C	vacuum	nil	nil
550° C	H_2S	strong ± 1/3 ⟨111⟩ maxima	

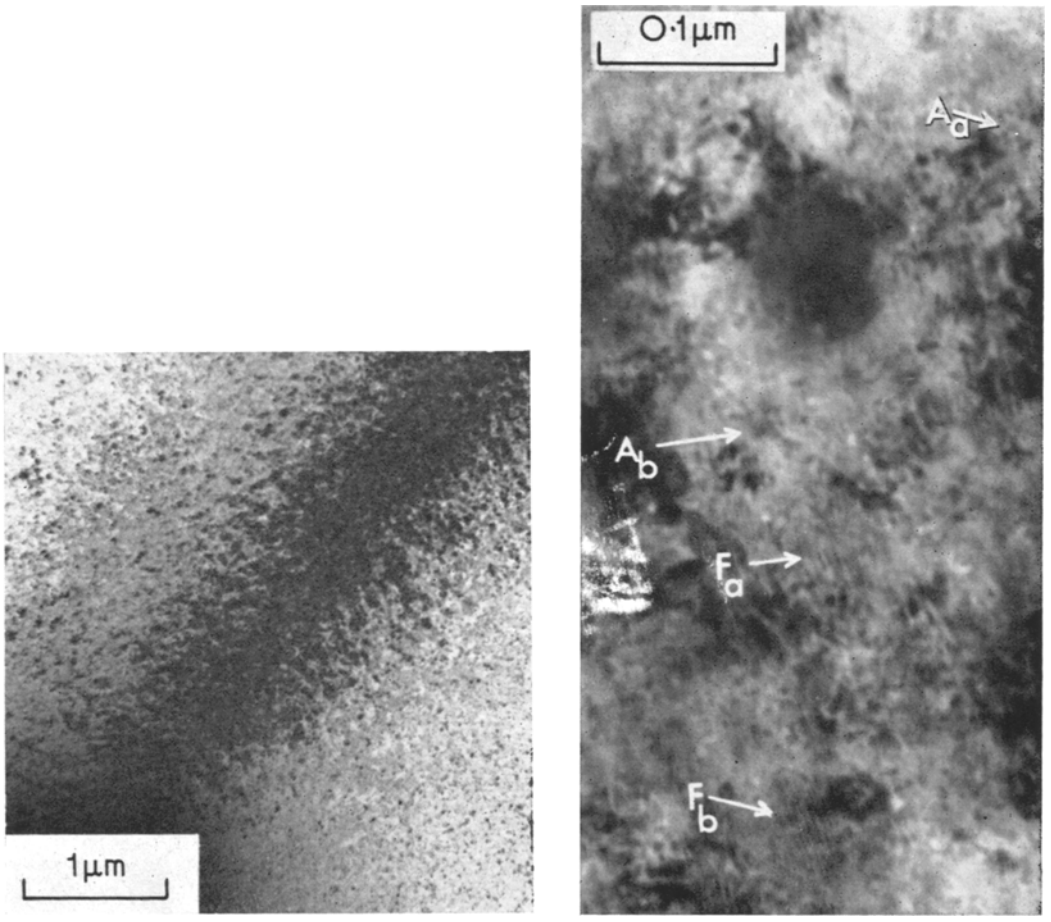

Figure 8 (a) A [220] bend extinction contour in a film of ZnS free of included grains. (b) Higher magnification micrograph of the edge of an extinction contour showing fringes marked F and arrays of dots marked A.

error, their spacings, were in agreement with the above hypothesis [7].

3.3. The Effect of Annealing

A number of epitaxial films of ZnS were grown under optimum conditions, floated off the NaCl substrates and picked up on gold grids. Their structures were checked. It was found that they were free of included grains and microtwins and contained only planar defects as described above. Several grids of ZnS films were then annealed under each of the sets of conditions listed in table I. The vacuum-annealing was carried out with the films put back into the vacuum system in which they were grown. The annealing in H_2S was carried out in a stream of the gas at a pressure of 1 atm. The annealing time was 1 h in all cases.

None of these treatments notably reduced the defect density in the films. Substantial diffusion took place in several cases as was shown by the formation of pits and by the appearance of intensity maxima at the $\pm$ 1/3 $\langle 1\,1\,1 \rangle$ positions along the streaks on the diffraction patterns. The appearance of these maxima indicated the formation of microtwins or possibly of included grains of the wurtzite-structure in the films. This was favoured by H_2S environments as table I shows.

Systematic analyses of these effects were not made as annealing did not appear likely to lead to an increased understanding of the planar defects nor to their elimination.

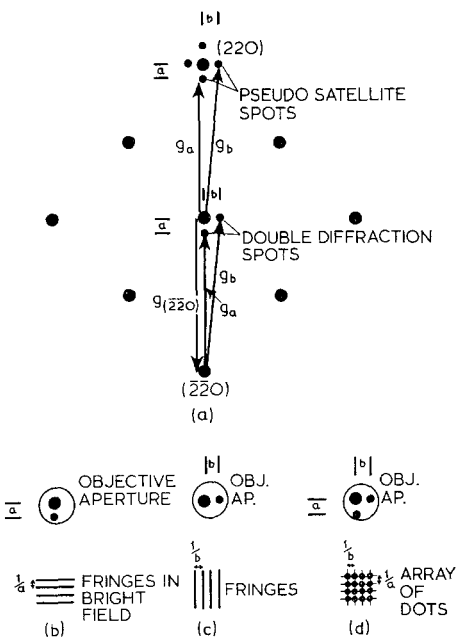

Figure 9 (a) Reciprocal lattice vector construction showing how satellite pseudo-spots can occur close to the spot from the direct beam by double diffraction; (b) and (c): when the objective aperture is placed to transmit the direct electron beam and a doubly diffracted beam, fringes are formed as indicated in the bright field images of the areas that diffract into the satellite pseudo-spot.

4. Discussion

4.1. Included Grains

The complete absence of wurtzite-structure included grains and of microtwins in the best films produced by focused electron beam evaporation [1, 2] constituted a considerable advance in structural perfection compared with previous work in the literature (reviewed in [8]).

The presence of only one type of included grain in the films prepared at non-optimum substrate temperatures, namely double- (or single-) positioned wurtzite is significant. The included grain structures observed in films of other II-VI compounds were quite different. Films of CdS evaporated onto cleavage faces of NaCl at low temperatures had the sphalerite structure and also contained only doubly-positioned wurtzite included grains. However CdS films grown on (100) NaCl at above optimum temperatures incorporated only wurtzite grains with basal {0001} planes parallel to the {111} planes of the film matrix [9]. Films of ZnTe evaporated onto NaCl were found to contain not only doubly-positioned wurtzite but microtwins and some {0001}-parallel-to-{111} wurtzite grains as well [5]. Thus the included grain structure of epitaxial films of II-VI compounds grown on the same substrates under very similar conditions varies markedly from one compound to another.

4.2. Planar Defects

That the defects were planar could be seen by viewing them edge-on (fig. 7). That they lay on {111} planes and were only a few atoms thick was proved by the occurrence of continuous streaks in the ⟨111⟩ directions in the diffraction patterns (fig. 4). These defects were also frequently triangular (fig. 6).

The typical appearance of the best films as grown (fig. 8) was dominated by the fine scale fringe and dot contrast due to the planar defects. It was shown above that this dot and fringe contrast arose through the interaction of the main (centre) beam of electrons and beams of electrons of neighbouring satellite pseudo-spots due to double diffraction (fig. 9).

These observations, however, do not suffice to establish the nature of the planar defects. Either stacking faults or thin planar precipitates, for example of ZnO, would be compatible with the evidence discussed above. Detailed studies of fringe contrast to determine the nature of the defects were impossible. This was because the defects were too small and overlapped too frequently in consequence of the thickness of the films and the large numbers of the defects occurring per unit volume. The film thickness of about 2000 to 2500 Å was the minimum for film continuity with this method of growth.

The annealing experiments were undertaken to help determine the nature of the defects. If these were stacking faults they might have annealed out in vacuum. If they were oxide platelets however they might not have, but might have been removed by annealing in H_2S under thermodynamic conditions in which sulphur should replace oxygen. In fact neither treatment eliminated the planar defects despite the fact that considerable diffusion occurred at the higher annealing temperatures, particularly in the presence of H_2S. Thus nothing was learned about the nature of the planar defects.

The fact that annealing in H_2S promoted structural changes is however significant. Annealing in H_2S is a method of filling sulphur vacancies in ZnS. This, and analogous processes for other

II-VI compounds, are widely used to reduce point defect densities and obtain standardised material for the measurement of physical properties. The occurrence of structural changes during these annealing treatments complicates the situation and may be one of the factors contributing to the irreproducibility of much work on II-VI compounds.

Acknowledgement

This work was supported in part by a CVD contract and is published by permission of the Ministry of Defence. One of us (J.M.W.) would like to thank the SRC for a Research Studentship.

References

1. B. A. UNVALA, J. M. WOODCOCK, and D. B. HOLT, *Brit. J. Appl. Phys.* **1** (1968) 11.
2. J. M. WOODCOCK and D. B. HOLT, *ibid* **2** (1969) 775.
3. D. W. PASHLEY and M. J. STOWELL, *Phil. Mag.* **8** (1963) 1605.
4. D. W. PASHLEY, M. J. STOWELL, and T. J. LAW, *Phys. Stat. Sol.* **10** (1965) 153.
5. D. B. HOLT, *J. Mater. Sci.* **4** (1969) 935.
6. P. S. AGGARWAL and A. GOSWAMI, *Indian J. Pure Appl. Phys.* **1** (1963) 366.
7. J. M. WOODCOCK, Ph.D. Thesis, Imperial College, 1968.
8. D. B. HOLT, *J. Mater. Sci.* **1** (1966) 280.
9. D. M. WILCOX and D. B. HOLT, *ibid* **4** (1969) 672.

Received 5 August and accepted 6 October 1969.